

## Article

# Influence of Organic Coating Thickness on Electrochemical Impedance Spectroscopy Response

Amanda Suellen de Paula <sup>1</sup>, Barbara Mitraud Aroeira <sup>1</sup>, Lucas Henrique de Oliveira Souza <sup>2</sup>,  
Alisson Cristian da Cruz <sup>1</sup>, Michele Fedel <sup>3</sup> , Brunela Pereira da Silva <sup>1,\*</sup>  and Fernando Cotting <sup>1</sup> 

- <sup>1</sup> Department of Chemical Engineering, Federal University of Minas Gerais, Belo Horizonte 31270-901, MG, Brazil; amandasuellenpaula@gmail.com (A.S.d.P.); bah.mitraud@gmail.com (B.M.A.); alissoncristian@gmail.com (A.C.d.C.); fernando@deq.ufmg.br (F.C.); henrrikelucas@gmail.com
- <sup>2</sup> Nuclear Technology Development Center, Minas Gerais, Belo Horizonte 31270-901, MG, Brazil;
- <sup>3</sup> Department of Industrial Engineering, University of Trento, Via Sommarive n. 9, 38123 Trento, Italy; michele.fedel@unitn.it
- \* Correspondence: brunelapereira@gmail.com

**Abstract:** Electrochemical Impedance Spectroscopy (EIS) is a non-destructive and powerful technique for characterizing corrosion systems, allowing for the evaluation of surface reaction mechanisms, mass transport, kinetic evolution, and corrosion levels of materials. This study aims to analyze the progression of corrosion using EIS, with a focus on the influence of organic coating thickness. For this purpose, layers of high-purity epoxy paint were applied to carbon steel plates with thicknesses of 50  $\mu\text{m}$ , 80  $\mu\text{m}$ , and 100  $\mu\text{m}$ . During the research, a direct correlation was observed between coating thickness and corrosion resistance, emphasizing the importance of identifying the optimal thickness for each type of coating. Additionally, it was found that thicker coatings may experience electrode penetration due to the tensions generated during deposition, resulting in cracks between the layers, while thinner coatings allow electrolyte penetration as they do not provide adequate protection to the base steel. Therefore, the 80  $\mu\text{m}$  thickness demonstrated greater resistance to corrosion compared to the other tested thicknesses.

**Keywords:** electrochemical impedance spectroscopy; organic coating; corrosion



**Citation:** de Paula, A.S.; Aroeira, B.M.; Souza, L.H.d.O.; da Cruz, A.C.; Fedel, M.; da Silva, B.P.; Cotting, F. Influence of Organic Coating Thickness on Electrochemical Impedance Spectroscopy Response. *Coatings* **2024**, *14*, 285. <https://doi.org/10.3390/coatings14030285>

Academic Editor: Jinyang Xu

Received: 18 January 2024

Revised: 8 February 2024

Accepted: 23 February 2024

Published: 27 February 2024



**Copyright:** © 2024 by the authors. Licensee MDPI, Basel, Switzerland. This article is an open access article distributed under the terms and conditions of the Creative Commons Attribution (CC BY) license (<https://creativecommons.org/licenses/by/4.0/>).

## 1. Introduction

Corrosion is defined as an electrochemical process in which a chemical reaction between material and components of the environment occurs, causing deterioration [1]. This electrochemical process is considered to be a problem worldwide. According to NACE International (National Association of Corrosion Engineers), it is estimated that corrosive processes and their consequences cost developed nations about 3%–5% of GDP or GNP [2].

In this context, carbon steel is a metal widely used in construction and industrial projects, such as marine engineering [3], due to its great chemical and mechanical properties and low price; however, despite its applicability, its fragility to corrosion is a major obstacle [4]. Its application in saline environments presents difficulty, as carbon steel has as its main cause of corrosion (specifically pitting corrosion), its fragility to contact with chloride ions [5,6] due to its aggressive character, which is attributed to its small ionic radius (which allows greater diffusion between the monolayers formed on the metal surface [6,7]).

Some techniques are used for corrosion prevention, such as the use of corrosion-resistant alloys, corrosion-resistant coatings, cathodic protection, corrosion inhibitors, salt scavengers, cathodic passivation, and regular washing [8].

The organic coatings industry has played a crucial role in protecting metal surfaces from corrosion. In this context, organic coating films are applied as a protective barrier, preventing the direct exposure of carbon steel to the corrosive environment [9]. Corrosion

protection using coatings is captivating because, beyond being cost-effective, it is one of the most flexible, efficient, and direct strategies available [8].

The composition of a coating varies according to the function it has to perform; however, one can generalize that a coating formulation should present a vehicle (resins and solvents), pigments and additives. The resins are responsible for forming the paint film, and the most widely used are epoxy resin, polyurethane, phenolic resin, furan resin and polyurea coatings, with epoxy being the most widely applied coating due to its distinct advantages (excellent adhesion, acid-base resistance, resistance to penetration and low shrinkage) [10]. In addition to the creation of barriers with the corrosive environment, organic coatings have mechanisms of cathodic protection (sacrifice) and inhibition (passive protection) [11].

Electrochemical techniques have been widely applied to evaluate the corrosion protection performance of polymer composite coatings, mainly using open circuit potential (OCP) measurements and electrochemical impedance spectroscopy (EIS) [12]. EIS has been used for the investigation of organic coatings for several reasons, such as to understand the protection mechanism of an organic coating, to predict the lifetime of the coating, and to detect changes in coating performance after exposure time [13–15]. In addition to the qualitative results, by modeling the spectra with a suitable equivalent circuit, the EIS is able to provide quantitative data on the electrical parameters of the coatings and their changes over time due to exposure to corrosive media, such as the coating capacitance ( $C_c$ ), which is associated with the amount of water absorbed during the initial stages of exposure to the electrolyte; the coating resistance ( $R_C$ ), which is related to the state of the coating, its additives or pigments, porosity and type of resin; the double layer capacitance ( $C_{dl}$ ), associated with the delaminated area of the coating; and the load transfer resistance ( $R_{ct}$ ), related to the susceptibility to corrosion of the substrate [13,16,17].

According to Shin and Shon (2010) [18], whose research focused on the effects of varying the thickness of an epoxy coating on the corrosion protection of carbon steel, there is an intrinsic relationship between the corrosion protection of the epoxy coating and its thickness, indicating that thicker coatings provide greater corrosion resistance compared to relatively thin coatings. In contrast, the conclusions of Zhang et al. (2021) [19], who investigated the influence of combining different paint film thicknesses on the corrosion resistance of steel sheets, suggest that increasing coating thickness can improve anticorrosive performance; however, this improvement is conditional on maintaining a certain primer thickness, as excessively thick coatings generally lead to greater internal stresses, resulting in cracks during use, which compromises anticorrosive performance.

Therefore, it is clear that the relationship between the thickness of the coating and its protective properties is not straightforward. The few previous studies that addressed the influence of coating thickness on corrosion protection present divergences, highlighting the pressing need for additional research in this area. Regarding this scenario, the present work aims to evaluate a coating system at different thicknesses, investigating the influence of this parameter on the electrochemical impedance spectroscopy response.

## 2. Experimental Details

### 2.1. System Preparation

Carbon steel 1020 plates ( $0.15\text{ m} \times 0.10\text{ m} \times 0.001\text{ m}$ ) were ground with silicon carbide paper, degreased with acetone, and dried in warm air as a pretreatment. In the test plates, a commercial epoxy coating (Interbond 998 PB, International Protective Coatings (Santo André/SP) Brazil) was applied using an extender to achieve different dry film thicknesses. The painting system consisted of a single coating layer, and the curing time was seven total days.

The thickness measurement of the paint systems after curing was performed using the magnetic field attenuation method with Homis brand equipment. Measurements were taken at seven points for each plate, and the average with standard deviation was calculated from these.

Upon complete curing of the coating, the area for the tests was delimited. PVC weldable gloves were glued onto the plates using neutral silicone adhesive (Vedacit), as shown in Figure 1.

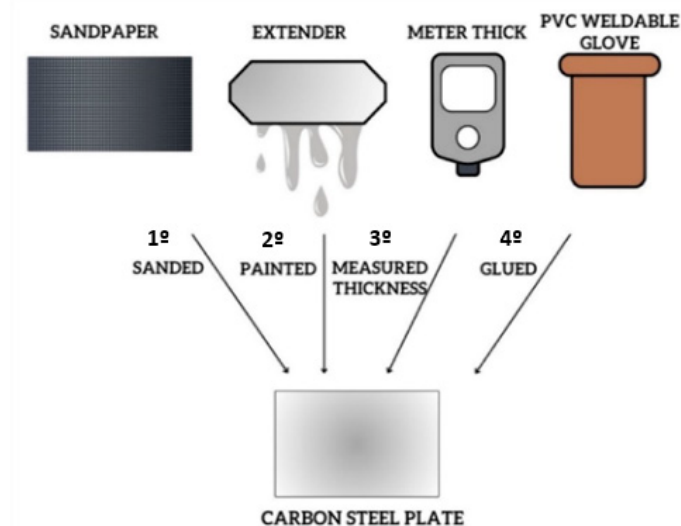


**Figure 1.** System preparation scheme steps: first the plate was sanded followed by the painting, then the thickness was measured, and finally the PVD was glued.

After the adhesive cured, a 3.5% NaCl electrolyte was added inside each glove for the electrochemical tests. Electrochemical impedance spectroscopy (EIS) tests were performed after 48 h, 7 days, 15 days, and 30 days of immersion.

## 2.2. Electrochemical Impedance Spectroscopy (EIS)

Electrochemical impedance spectroscopy measurements were conducted on the carbon steel plates coated with epoxy coatings using a Gamry Reference 620 potentiostat - Gamry Instruments (Warminster, PA, USA). The painted carbon steel plate was the working electrode, with an exposed area of 8 cm<sup>2</sup>. An Ag/AgCl(KCl 3M) reference electrode (Analion) and a platinum wire counter electrode were also used. The frequency range was from 100 kHz to 10 mHz, with a sinusoidal perturbation of 20 mV (RMS) × OCP, and 10 measurements per decade of frequency were acquired. EIS measurements were performed in triplicate. The experimental setup is shown in Figure 2.



**Figure 2.** Electrochemical cell.

Each specimen had its behavior studied via EIS in order to verify the influence of thickness and time variables on the specimens. The data were processed in the Origin 8.0 software.

### 2.3. Pull-Off Adhesion Test

For the characterization of adhesion test of painting systems, the PosiTest At-DeFeslko Corporation (Ogdensbur, NY, USA) equipment was used, and measurements were taken in the immersed and the non-immersed regions. The samples were sanded before fixing the pins to eliminate the gloss. The 20 mm diameter pins were fixed to the plates using a 24 h curing epoxy adhesive, and the test used an F-8 piston. The results were analyzed and discussed according to ASTM D4541-22 [20].

### 2.4. Scanning Electron Microscopy (SEM)/Energy Dispersive X-ray Spectroscopy (EDS)

The SEM/EDS images were obtained by the Scanning Electron Microscope—FEI Quanta 200 Field Emission Gun (FEG)—FEI Company (Hillsboro, OR, USA), located at the Microscopy Center of the Federal University of Minas Gerais (UFMG).

The images of secondary electrons (SE) were obtained using the ETD detector.

Regarding the EDS analysis, the detector was the silicon drift detector (SDD) type, with an energy resolution of 139 eV. The software used was the Bruker ESPRIT 2.1.

Previously in the analysis, the samples were metalized with carbon element.

## 3. Results and Discussion

The experimental thickness data for each coating are presented in Table 1. The table contains average and standard deviation, and coefficient of variation data for the thickness of each coating, performed in triplicate (C50, C80, and C100). The values 50, 80, and 100 represent the height of the coating layer in micrometers, which were defined as the study objective.

**Table 1.** Thickness of the samples studied.

Samples	C50	C80	C100
Average [ $\mu\text{m}$ ]	52.77	81.94	104.40
Standard Deviation [ $\mu\text{m}$ ]	2.43	2.43	6.43
Coefficient of Variation [%]	4.6	3.0	6.2

The decision to adopt extenders for the application of the coatings took into consideration the coating itself, which has a high solids content, resulting in minimal thickness loss compared to the wet film, and aimed to achieve a uniform thickness across the entire plate. Proper application of a coating results in a defect-free film, good appearance, and an extended service life for corrosion protection.

The coatings applied during this study were found to be homogeneous in terms of thickness and free of visible defects. The application using extenders has a peculiarity compared to other application methods, as it occurs in a single layer. This means that the presence of defects, such as high porosity, becomes more likely and can affect the impedance results obtained. In Figure 3, it is possible to observe the secondary electron images using Scanning Electron Microscopy (SEM)—FEI Company (Hillsboro, OR, USA) of the surface of the produced materials. As mentioned earlier, the presence of porosity on the material's surface is evident. It was noticeable that, as the thickness decreased, the porosity increased, as can be observed in Figure 3a,d. Figure 3c,d represent a thickness of 100  $\mu\text{m}$  at different magnitudes ( $50\times$  and  $500\times$ , respectively), and through them it is possible to verify that the number of pores is smaller when compared to Figure 3a,b, which represent thicknesses C50 and C80, respectively.



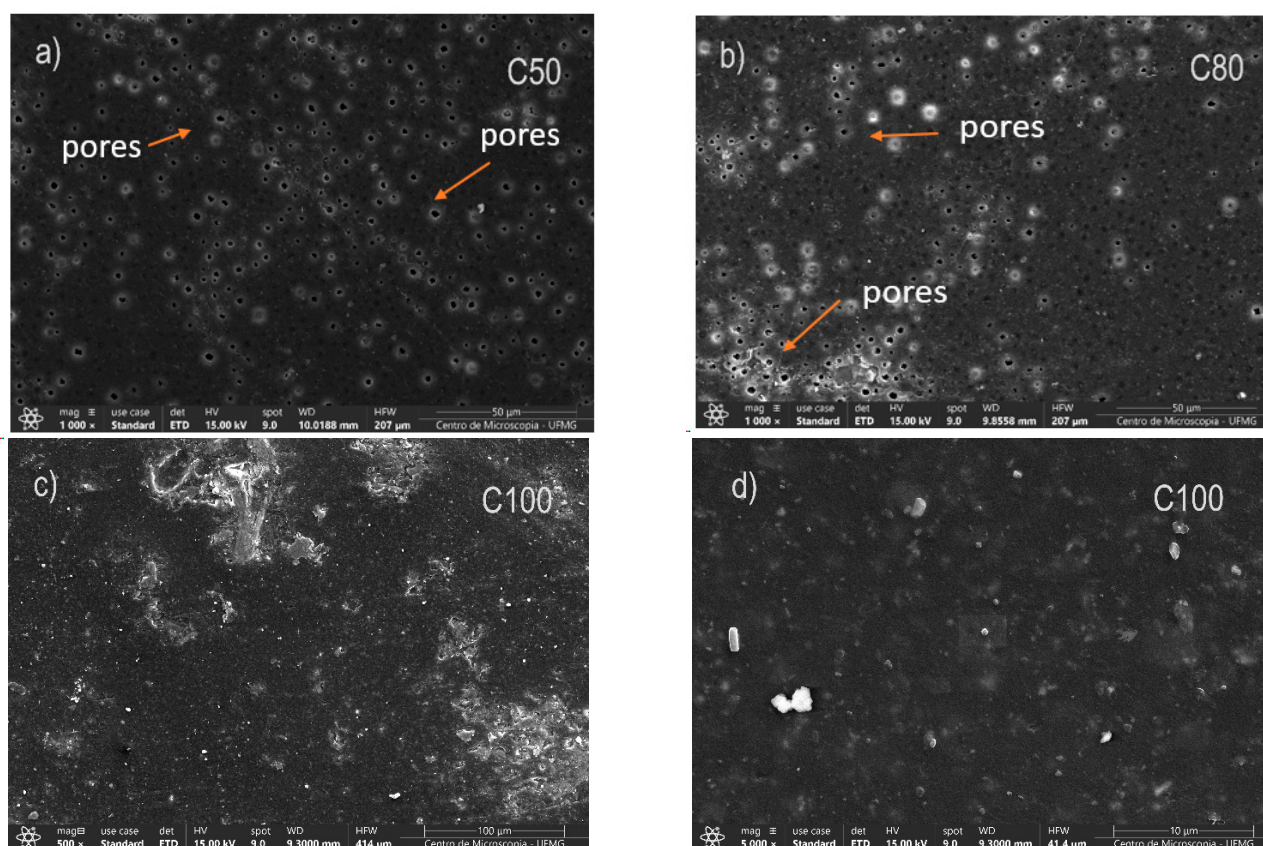


**Figure 3.** Scanning Electron Microscopy (SEM) of the surface of samples (a) C50, (b) C80, (c,d) C100.

Other discontinuities such as cracks and deformations were not visualized, and also not detected in SEM images, which can indicate that the coating pores are the more prominent defect found in the painting system.

Upon analyzing Figure 4, one can observe the thicknesses achieved through the application with the extender. It is evident that the thinner the thickness, the greater the challenges in achieving uniform paint application, directly impacting the obtained thicknesses, as can be seen through SEM. In Figure 5, it is possible to observe the chemical map of the paint applied to the metal surface.

In the Supplementary Material, Figures 5, S1 and S2 show the maps of the separate chemical compounds found in the commercial epoxy coating, which are aluminum (Al), magnesium (Mg), oxygen (O), silicon (Si), and titanium (Ti). The sodium (Na) and chlorine (Cl) appeared in Figure 5 because the samples were immersed in the NaCl solution and the EDS was then realized.

Electrochemical Impedance Spectroscopy (EIS) was performed after different immersion time intervals of materials with the specified thicknesses in Table 1 in a 3.5% NaCl medium: 48 h, 7 days, 15 days, 30 days, and 60 days. Figure 6 demonstrates the behavior of the studied coatings at the described immersion times through Bode diagrams.

Analyzing first the thickness of 50  $\mu\text{m}$  (C50), it was observed that its resistance decreased significantly over the immersion time in the NaCl medium, showing a sharp decline, particularly when comparing the 48 h and 30 d periods, represented by Figure 6a,d. However, after a period of 60 days, as evidenced in Figure 6d, there was a slight increase in resistance.

After analyzing more than 300 paint systems, Bacon et al. (1948) [21] identified a direct correlation between the resistance of coatings and their ability to protect steel against corrosion. According to the authors, coatings that maintain a resistance above  $10^8 \text{ ohm}\cdot\text{cm}^2$  provide good corrosion protection. In the range between  $10^6$  and  $10^8 \text{ ohm}\cdot\text{cm}^2$ , the behavior of the coatings varies, while values below  $10^6 \text{ ohm}\cdot\text{cm}^2$  indicate low corrosion protection.

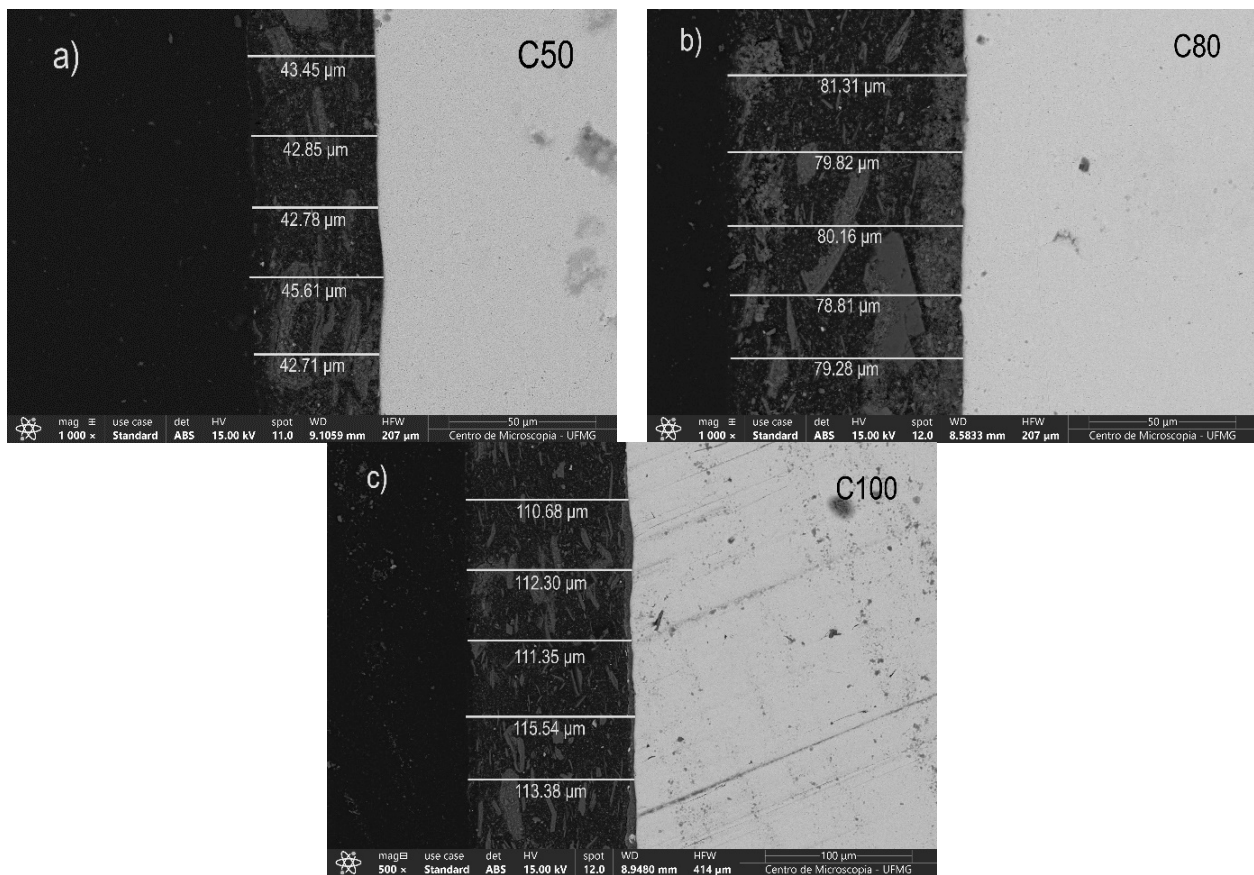


**Figure 4.** Scanning Electron Microscopy (SEM) of the thickness of samples (a) C50, (b) C80, (c) C100.

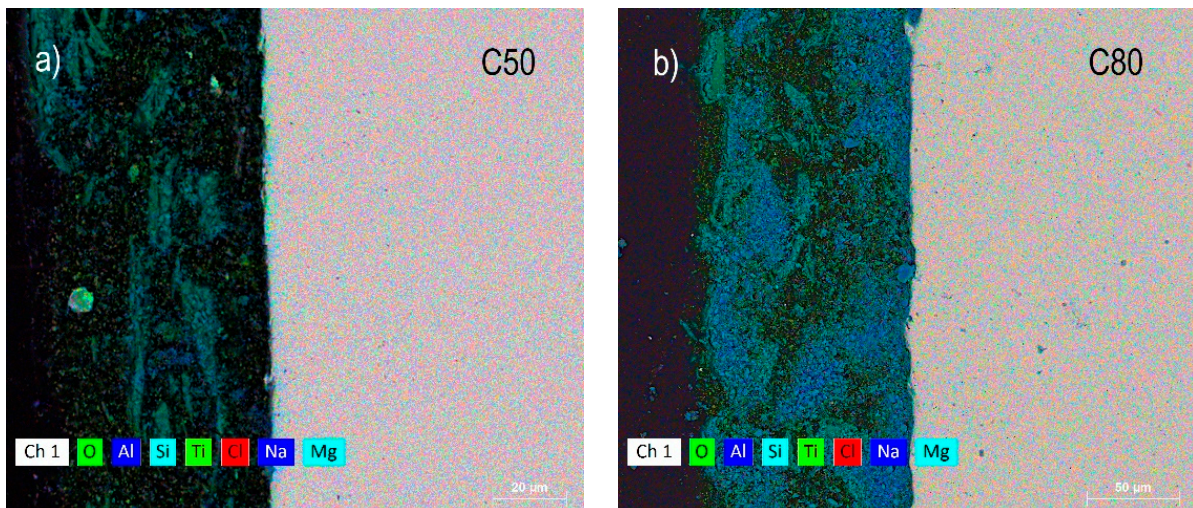


**Figure 5.** Chemical maps of the commercial epoxy coating for the samples (a) C50, (b) C80,

Therefore, the thickness of 50 μm after 60 days of immersion can still be considered a viable option, as it is slightly above the  $10^8$  ohm·cm<sup>2</sup> threshold specified by Bacon et al. (1948) [21].

The thickness of 80 μm, on the other hand, exhibits lower impedance than the 100 μm thickness in the first 48 h and 7 days of immersion. However, after 15 days, the resistance of the 80 μm thickness starts to exceed that of the 100 μm thickness, and after 30 days, a significant overtaking occurs.



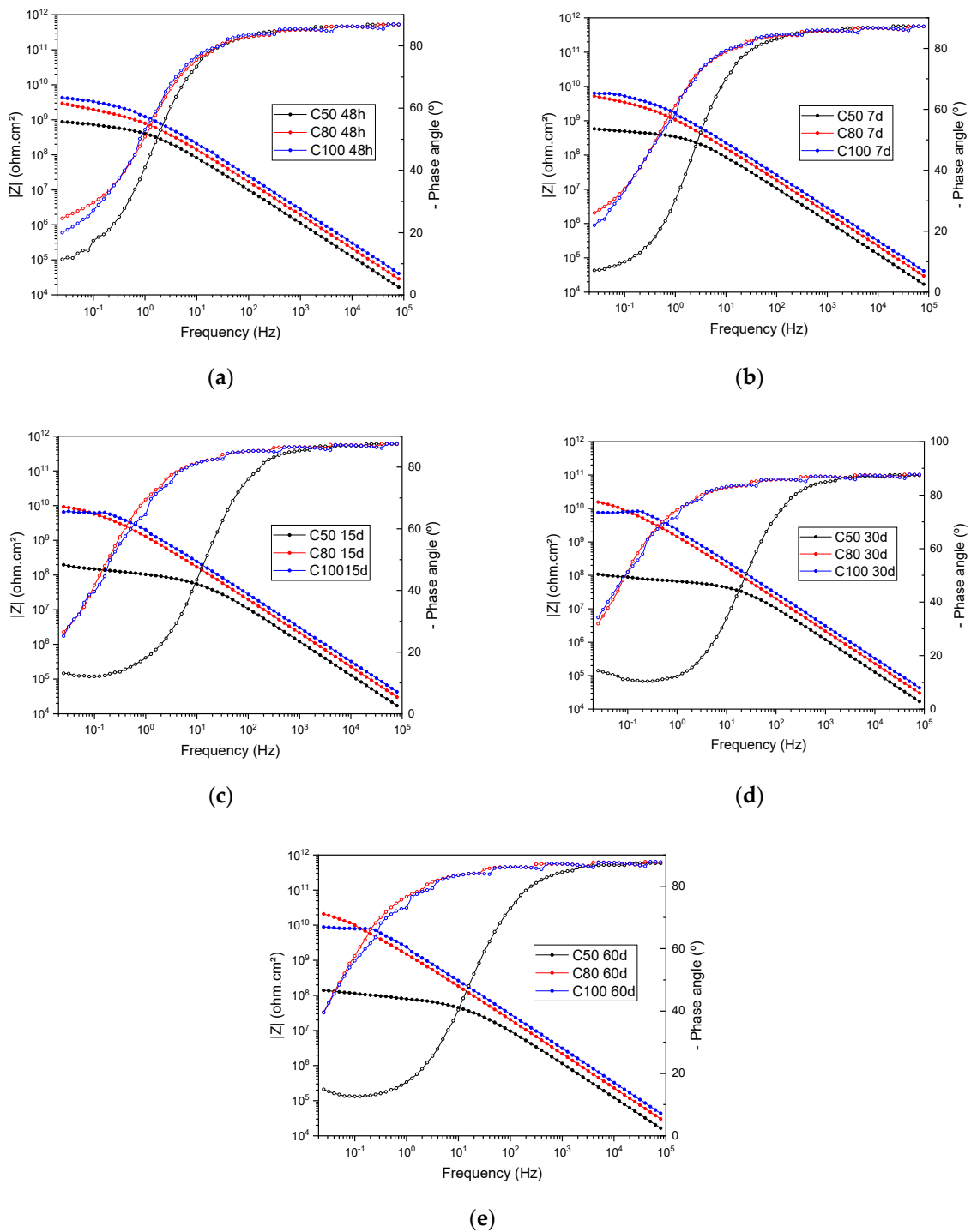


**Figure 6.** Bode diagrams for coating thicknesses of 50  $\mu\text{m}$ , 80  $\mu\text{m}$ , and 100  $\mu\text{m}$  with the following immersion times in 3.5% NaCl solution: (a) 48 h, (b) 7 days, (c) 15 days, (d) 30 days and (e) 60 days.

Finally, the 100  $\mu\text{m}$  thickness initially exhibits higher resistance than the other thicknesses in the first 48 h. However, this resistance gradually declines after 7 days and is ultimately surpassed by the 80  $\mu\text{m}$  thickness after 15 days of immersion.

According to Bacon et al. (1948) [21], some coatings may initially show a decrease in resistance followed by a sudden increase. Generally, after this increase, the value of  $\log R$  may remain unchanged, increase, or decrease in the high resistance region, as is the case here. The authors describe this trend as a “repair trend”. However, to some extent, these variations in coating resistance can be attributed to processes occurring at the

metal-coating interface. These processes begin with an initial decrease in resistance due to water permeation and the transport of conductive constituents within the coating. As a result, corrosion product barriers are formed at the metal-coating interface and possibly in the pores and interstices near this interface. These barriers prevent the passage of conductive particles to the metal surface, which leads to an increase in resistance. While this phenomenon is most pronounced in the 80  $\mu\text{m}$  thickness, it is also noticeable in the 100  $\mu\text{m}$  thicknesses, particularly when examining initial immersion times (from 48 h to 7 d and after, to 15 d). These cases reveal a subtle rise in resistance, as illustrated in Figure 7. Analyzing the image, it is possible to visualize that, at the beginning, the  $|Z|$  modulus increased to the sample C80 and C100, proving the phenomenon of “repair trend”.

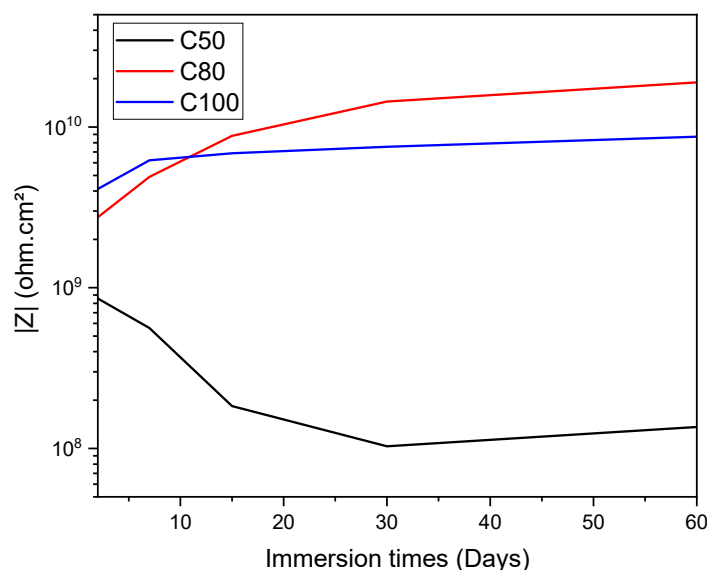


**Figure 7.** Relationship of resistance as a function of time for thicknesses of 50  $\mu\text{m}$ , 80  $\mu\text{m}$ , and 100  $\mu\text{m}$ .

In Figure 7 we observe the variation of impedance (at a frequency of 30 mHz) in the coating samples with different thicknesses (C50, C80, and C100) during the 60 days of immersion in a NaCl medium.

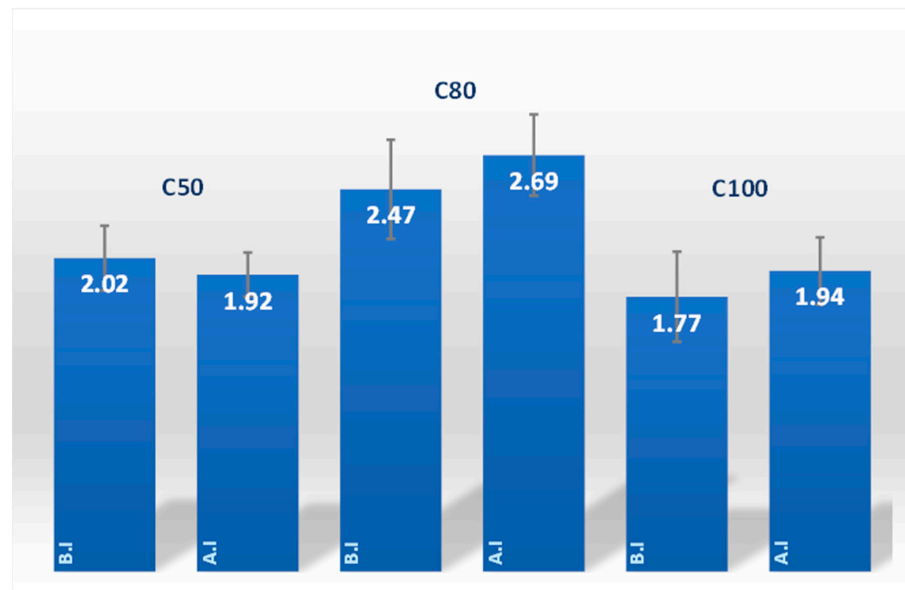
As can be observed, although at shorter immersion times there is a higher corrosion resistance in the material with greater thickness (C100), for longer times, above 10 days, the 80  $\mu\text{m}$  thickness exhibits higher resistance. Additionally, by the slope of the curves, it can be seen that the corrosion resistances of the C80 and C100 materials increase with longer immersion times.

This behavior can be explained by the fact that thicker coatings typically allow electrolyte penetration due to the stresses generated during coating deposition and the formation of cracks between different layers, whereas thinner coating samples allow electrolyte penetration through the coating because it is not thick enough to properly protect the base steel [22]. Thus, the correlation between coating thickness and corrosion resistance is directly proportional, and it is necessary to identify the optimal thickness for each coating.

Evaluating the efficiency of the coatings, all samples showed adequate performance for immersion times of up to 60 days in a medium with 3.5% NaCl. The impedance modules for samples C80 and C100 showed magnitude in the order of  $|Z|_{0.03\text{Hz}} \sim 10^9 \text{ ohm}\cdot\text{cm}^2$ , a value above  $10^8 \text{ ohm}\cdot\text{cm}^2$ , which indicates good anticorrosive activity for an organic coating. The C50 sample, on the other hand, presented impedance modulus values in the order of  $|Z|_{0.03\text{Hz}} \sim 10^8 \text{ ohm}\cdot\text{cm}^2$ , and thus presents a lower performance for anticorrosive protection when compared to the other samples.

The pull-off strength results obtained from the test in non-immersed and immersed in NaCl 3.5% solution area are presented in Figure 8 for thickness conditions of 50  $\mu\text{m}$ , 80  $\mu\text{m}$ , and 100  $\mu\text{m}$ .



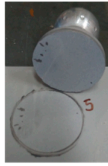
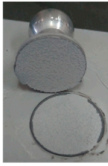
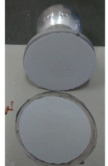
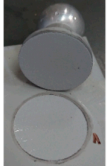




**Figure 8.** Pull-off adhesion tests of coated samples with thicknesses of 50 μm, 80 μm, and 100 μm in areas before (B.I) and after (A.I) immersion of 60 days in NaCl 3.5% solution.

By the average pull-off strength values, we can affirm that the coating with an 80 μm thickness exhibited the best adhesion properties, followed by the 50 μm and 100 μm samples. The strength values are closely linked to the surface preparation of metal plates, ensuring the presence of an adequate roughness profile to facilitate coating adhesion.

In addition to the strength values, the pull-off test provides a qualitative result regarding the type of failure observed during coating detachment. The characterization of the obtained failure is determined based on the occurrence of adhesive failures, which take place between different layers, and cohesive failures, which occur within the same layer. The types of failures observed in the samples with varying thicknesses are shown in Figure 9.

Samples	Types of failure	
	Without immersion	With immersion
C50	 <p>100% cohesive paint failure</p>	 <p>99% cohesive paint failure 1% adhesive cohesive failure</p>
C80	 <p>97% cohesive paint failure 3% adhesive cohesive failure</p>	 <p>100% cohesive paint failure</p>
C100	 <p>100% cohesive paint failure</p>	 <p>100% cohesive paint failure</p>

**Figure 9.** Types of failures observed after pull-off test for coatings with thicknesses of 50 μm, 80 μm, and 100 μm in areas with and without immersion in NaCl 3.5% solution.

The coatings were applied in a single layer, and the samples predominantly exhibited cohesive paint failure. This result indicates the strong adhesion of the coating to the metallic substrate.

#### 4. Conclusions

(1) The electrochemical impedance spectroscopy tests showed that C80 was the material with the epoxy coating thickness with the highest corrosion resistance in NaCl electrolyte after sixty days of immersion. We observed that, in the 24 h of immersion, the impedance values in the low frequency region present a correlation with the thickness of the applied coating in order to increase the modulus value for the thicker samples. After 10 days of immersion, this behavior changed so that sample C80 presented higher modulus values followed by sample C100 and finally C50. Thin coatings facilitate the penetration of the electrolyte and, consequently, its contact with the metal surface, while thick coatings may present deformations or cracks during their preparation that also act by exposing the base metal to the electrolyte (it is necessary for these cases to have efficient quality control during the application step).

(2) Regarding SEM/EDS technique, the thickness of the samples C50, C80 and C100 was also confirmed by secondary electron (SE) images. The chemical element maps of the coating were showed by EDS analysis, obtaining the main compounds of the commercial epoxy coating

(3) The pull-off adhesion test proved that the sample C80 exhibited the highest tensile stretch value, indicating a strong correlation between adhesion and the performance in the EIS tests

Finally, the electrochemical impedance spectroscopy technique proved to be a suitable tool to differentiate the  $|Z|$  values, and also the corrosion development, of carbon steel sheets painted with different organic coating thickness. A clear correlation between the impedance modulus value and the porosity/thickness of the coating was proven.

Also, the SEM technique confirmed the achievement of the desired thicknesses. The pull-off test confirmed the good adhesion of the coating to the metallic substrate in samples with varying thicknesses, with the highest pull-off strength being recorded in the 80  $\mu\text{m}$  thick sample.

**Supplementary Materials:** The following supporting information can be downloaded at: <https://www.mdpi.com/article/10.3390/coatings14030285/s1>, Figure S1: Chemical maps of each element in the commercial epoxy coating for the sample C50 (50  $\mu\text{m}$  thicknesses); Figure S2: Chemical maps of each element in the commercial epoxy coating for the sample C80 (80  $\mu\text{m}$  thicknesses).

**Author Contributions:** Conceptualization, A.S.d.P., B.M.A., L.H.d.O.S., A.C.d.C., B.P.d.S. and F.C.; Methodology, A.S.d.P., B.M.A., L.H.d.O.S. and A.C.d.C.; Validation, A.S.d.P., B.M.A., L.H.d.O.S. and A.C.d.C.; Formal Analysis, A.S.d.P., B.M.A., L.H.d.O.S. and A.C.d.C.; Investigation, A.S.d.P., B.M.A., L.H.d.O.S. and A.C.d.C.; Resources, F.C.; Writing—Original Draft Preparation, A.S.d.P., B.M.A., L.H.d.O.S. and A.C.d.C.; Writing—Review and Editing, B.P.d.S., M.F. and F.C.; Supervision, B.P.d.S. and F.C.; Project Administration, F.C.; Funding Acquisition, F.C. All authors have read and agreed to the published version of the manuscript.

**Funding:** The present work is thankful to CAPES—Brazil (Coordination for the Improvement of Higher Education Personnel), CNEN—Brazil (The National Nuclear Energy Commission) and CNPq—Brazil (Nacional Council for Scientific and Technological Development, project # 312552/2022-0).

**Institutional Review Board Statement:** Not applicable.

**Informed Consent Statement:** Not applicable.

**Data Availability Statement:** The data presented in this study are available on request from the corresponding author.

**Conflicts of Interest:** The authors declare no conflicts of interest.

## References

1. Darvell, B.W. Corrosion—Chapter 13. In *Materials Science for Dentistry*, 10th ed.; Elsevier: Amsterdam, The Netherlands, 2018; pp. 382–398. [\[CrossRef\]](#)
2. Umoren, S.A.; Solomon, M.M.; Saji, V.S. Chapter 3—Basic Concepts of Corrosion. In *Polymeric Materials in Corrosion Inhibition*; Elsevier Science: Amsterdam, The Netherlands, 2022.
3. Cai, F.; Huang, Y.; Xing, S.; Xu, Y.; Zhao, X.; Wang, X.; Wang, Z.; Ringsberg, J.W. Characteristics and Mechanisms of Low-Alloy High-Strength Steel Corrosion Behavior under Barnacle Adhesion Based on a Comparison Experiment. *Corros. Sci.* **2023**, *217*, 111146. [\[CrossRef\]](#)
4. Mohammed, H.K.; Jafar, S.A.; Humadi, J.I.; Sehgal, S.; Saxena, K.K.; Abdullah, G.H.; Saeed, L.I.; Salman, M.S.; Abdullah, W.S. Investigation of Carbon Steel Corrosion Rate in Different Acidic Environments. *Mater. Today Proc.* **2023**. [\[CrossRef\]](#)
5. Mahjani, M.G.; Neshati, J.; Masiha, H.P.; Jafarian, M. Electrochemical Noise Analysis for Estimation of Corrosion Rate of Carbon Steel in Crude Oil. *Anti-Corros. Methods Mater.* **2007**, *54*, 27–33. [\[CrossRef\]](#)
6. Macedo, R.G.M.d.A.; Marques, N.d.N.; Tonholo, J.; Balaban, R.d.C. Water-Soluble Carboxymethylchitosan Used as Corrosion Inhibitor for Carbon Steel in Saline Medium. *Carbohydr. Polym.* **2019**, *205*, 371–376. [\[CrossRef\]](#) [\[PubMed\]](#)
7. Heakal, F.E.T.; Fouda, A.S.; Radwan, M.S. Some New Thiadiazole Derivatives as Corrosion Inhibitors for 1018 Carbon Steel Dissolution in Sodium Chloride Solution. *Int. J. Electrochem. Sci.* **2011**, *6*, 3140–3163. [\[CrossRef\]](#)
8. Honarvar Nazari, M.; Zhang, Y.; Mahmoodi, A.; Xu, G.; Yu, J.; Wu, J.; Shi, X. Nanocomposite Organic Coatings for Corrosion Protection of Metals: A Review of Recent Advances. *Prog. Org. Coat.* **2022**, *162*, 106573. [\[CrossRef\]](#)
9. Sørensen, P.A.; Kiil, S.; Dam-Johansen, K.; Weinell, C.E. Anticorrosive Coatings: A Review. *J. Coat. Technol. Res.* **2009**, *6*, 135–176. [\[CrossRef\]](#)
10. Li, H.; Zhang, Q.H.; Meng, X.Z.; Liu, P.; Wu, L.K.; Cao, F.H. A Novel Cerium Organic Network Modified Graphene Oxide Prepared Multifunctional Waterborne Epoxy-Based Coating with Excellent Mechanical and Passive/Active Anti-Corrosion Properties. *Chem. Eng. J.* **2023**, *465*, 142997. [\[CrossRef\]](#)
11. Caraguay, S.J.; Pereira, T.S.; Cunha, A.; Pereira, M.; Xavier, F.A. The Effect of Laser Surface Textures on the Adhesion Strength and Corrosion Protection of Organic Coatings—Experimental Assessment Using the Pull-off Test and the Shaft Load Blister Test. *Prog. Org. Coat.* **2023**, *180*, 107558. [\[CrossRef\]](#)
12. Li, J.; Ecco, L.; Fedel, M.; Ermini, V.; Delmas, G.; Pan, J. In-Situ AFM and EIS Study of a Solventborne Alkyd Coating with Nanoclay for Corrosion Protection of Carbon Steel. *Prog. Org. Coat.* **2015**, *87*, 179–188. [\[CrossRef\]](#)
13. Ecco, L.G.; Li, J.; Fedel, M.; Deflorian, F.; Pan, J. EIS and in Situ AFM Study of Barrier Property and Stability of Waterborne and Solventborne Clear Coats. *Prog. Org. Coat.* **2014**, *77*, 600–608. [\[CrossRef\]](#)
14. Moreto, J.A.; Marino, C.E.B.; Bose Filho, W.W.; Rocha, L.A.; Fernandes, J.C.S. SVET, SKP and EIS Study of the Corrosion Behaviour of High Strength Al and Al-Li Alloys Used in Aircraft Fabrication. *Corros. Sci.* **2014**, *84*, 30–41. [\[CrossRef\]](#)
15. Suay, J.J.; Rodríguez, M.T.; Razaq, K.A.; Carpio, J.J.; Saura, J.J. The Evaluation of Anticorrosive Automotive Epoxy Coatings by Means of Electrochemical Impedance Spectroscopy. *Prog. Org. Coat.* **2003**, *46*, 121–129. [\[CrossRef\]](#)
16. Calderón-gutierrez, J.A.; Bedoya-lora, F.E. Barrier Property Determination and Lifetime Prediction By Electrochemical Impedance Spectroscopy of a High Performance Organic Coating. *Dyna* **2014**, *183*, 97–106. [\[CrossRef\]](#)
17. Zhao, X.; Qi, Y.; Zhang, Z.; Li, K.; Li, Z. Electrochemical Impedance Spectroscopy Investigation on the Corrosive Behaviour of Waterborne Silicate Micaceous Iron Oxide Coatings in Seawater. *Coatings* **2019**, *9*, 415. [\[CrossRef\]](#)
18. Shin, A.S.; Shon, M.Y. Effects of Coating Thickness and Surface Treatment on the Corrosion Protection of Diglycidyl Ether Bisphenol-A Based Epoxy Coated Carbon Steel. *J. Ind. Eng. Chem.* **2010**, *16*, 884–890. [\[CrossRef\]](#)
19. Zhang, H.; Xue, B.; Wang, C.; Yue, Y.; Luo, J.; Yan, R. Research on the Influence of Different Paint Film Thickness Combination on Corrosion Resistance of Sandblasting Steel Plate. *J. Phys. Conf. Ser.* **2021**, *1965*, 012106. [\[CrossRef\]](#)
20. *ASTM D4541-22*; American Society of Testing Materials and Standard Test Method for Pull-Off Strength of Coatings Using Portable Adhesion Tester. ASTM: West Conshohocken, PA, USA, 2022.
21. Bacon, R.C.; Smith, J.J.; Rugg, F.M. Electrolytic Resistance in Evaluating Protective Merit of Coatings on Metals. *Ind. Eng. Chem.* **1948**, *40*, 161–167. [\[CrossRef\]](#)
22. Guilemany, J.M.; Fernández, J.; Delgado, J.; Benedetti, A.V.; Climent, F. Effects of Thickness Coating on the Electrochemical Behaviour of Thermal Spray Cr<sub>3</sub>C<sub>2</sub>-NiCr Coatings. *Surf. Coat. Technol.* **2002**, *153*, 107–113. [\[CrossRef\]](#)

**Disclaimer/Publisher’s Note:** The statements, opinions and data contained in all publications are solely those of the individual author(s) and contributor(s) and not of MDPI and/or the editor(s). MDPI and/or the editor(s) disclaim responsibility for any injury to people or property resulting from any ideas, methods, instructions or products referred to in the content.